Journal of the Korean Society of Marine Engineering, Vol.32, No.3, pp.404~412, 2008(ISSN 1226-9549)

Investigation on the Internal Flow Characteristics of the Low Specific Speed Centrifugal Pump with Circular Casing

Young-Do Choi†

(Manuscript : Received March 20, 2008 ; Revised May 9, 2008)

Abstract : As a suitable volute configuration in the range of low specific speed, circular casing is suggested in this study. The internal flows in a centrifugal pump with the circular and spiral casings are measured by PIV and analyzed by CFD. The results show that the head and efficiency of the pump by a circular casing of very small radius are almost same as those by the spiral casing. Even at the best efficiency point, the internal flow of the pump by circular casing is asymmetric, and vortex and strong secondary flow occurs in the impeller passage. The radial velocity becomes higher remarkably only near the region of the discharge throat. The flow in the impeller outlet is strongly controlled by the circular casing because the velocity distribution almost does not affected by the position of the impeller blades.

Key words : Centrifugal pump, Low specific speed, Internal flow, Spiral casing, Circular casing

1. Introduction

As the specific speed becomes lower, the efficiency of the centrifugal pump decreases rapidly[1]. Kurokawa et al.[2],[3] have studied on the performance of centrifugal pump for the low specific speed, and have made clear the effects of impeller and casing parameters on the performance near the specific speed range of n_s=60 [m, m^3/min, min^{-1}]. Moreover, new study result was found that increase of leakage and disc friction in the pump can increase efficiency in the range of very low specific speed, which is a contrary result to the conventional theory in the range of normal specific speed[4]. Also, semi-open type impeller is suitable because of their good stability, comparing with the closed type impeller in the range of very low specific speed[5],[6].

As specific speed becomes lower, the spiral angle becomes very small. Therefore, manufacture of the spiral casing needs very high accuracy and thus, manufacturing cost becomes higher considerably.

Choi et al.[7] have suggested circular casing in the range of very low specific speed, and conducted experimental study to improve the pump performance.

† Corresponding Author(Korea Maritime University, Industry-Academic Cooperation Foundation, E-mail:ydchoi@pivlab.net, Tel: 051)410-4940)

The purpose of this study is aimed to examine the characteristics of the internal flow as well as the performance of the pump with circular casing in order to achieve basic knowledge of the internal flow field.

PIV(Particle Image Velocimetry) and CFD(Computational Fluid Dynamics) are adopted for the investigation of the internal flow.

2. Experimental and numerical methods

2.1 Experimental apparatus

Fig. 1 shows the cross-sectional view of a test pump. The channel from the inlet of the impeller to the outlet of the casing is made as a two-dimensional configuration between two pieces of flat plates. The front wall and side walls of the casing in the test section are made of transparent acrylic resin for the visualization and PIV(Particle Image Velocimetry) measurement.

Fig. 2(a) shows the schematic view of the test impeller. This impeller is the semi-open type, whose outlet angle of the blade is β_2 = 30 degree. Tip clearance ratio is c/b_2 = 0.125, while c is tip clearance between front casing wall and upper wall on the impeller blade. Depth of the impeller blade at impeller outlet is b_2=8mm. The rotational speed of the axis is n=900rpm.

The shapes of test casing are shown in Fig. 2(b). The casing type can be easily changed and modified from the test pump. The ratio of cross-sectional area at the discharge throat A_3 of the casing is A_3/A_2 = 0.056 for all casings, while A_2 is cross-sectional area at the outlet of impeller passage. These casings are designed to be the specific speed of n_s=100[m, m^3/min, min^{-1}] at the matching point between impeller and casing.

Two types of discharge channel are used as shown in Fig. 2(b). One of the channels is expanded from the discharge throat to the end of the channel with the expansion angle of 8degree. The other channel has a straight shape.

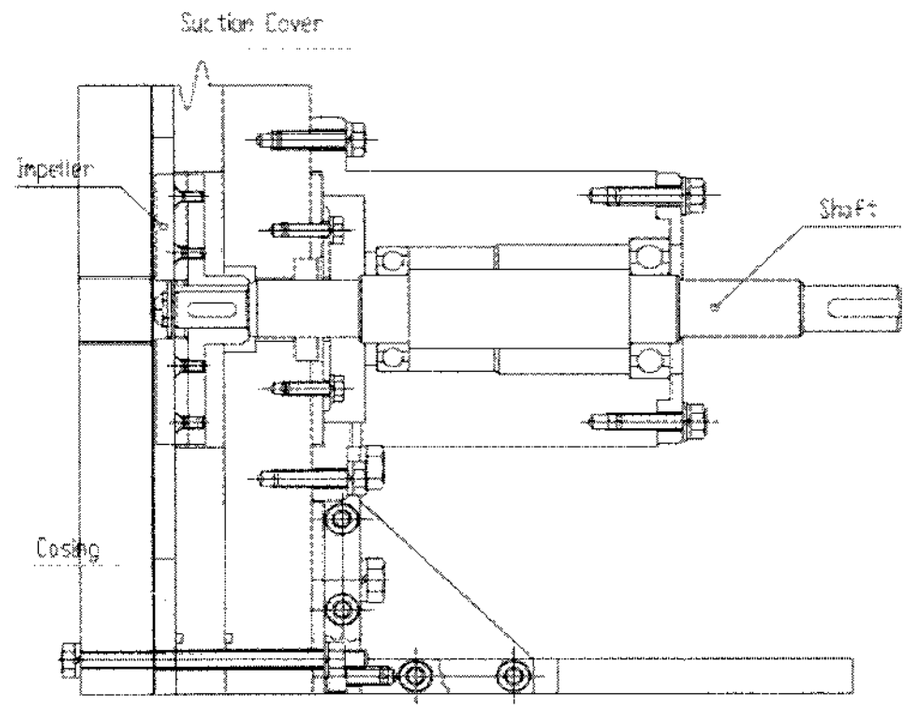

Fig. 1 Cross-sectional view of test pump

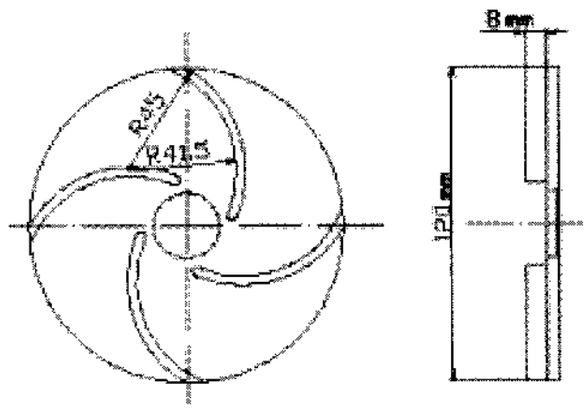

(a) Test impeller

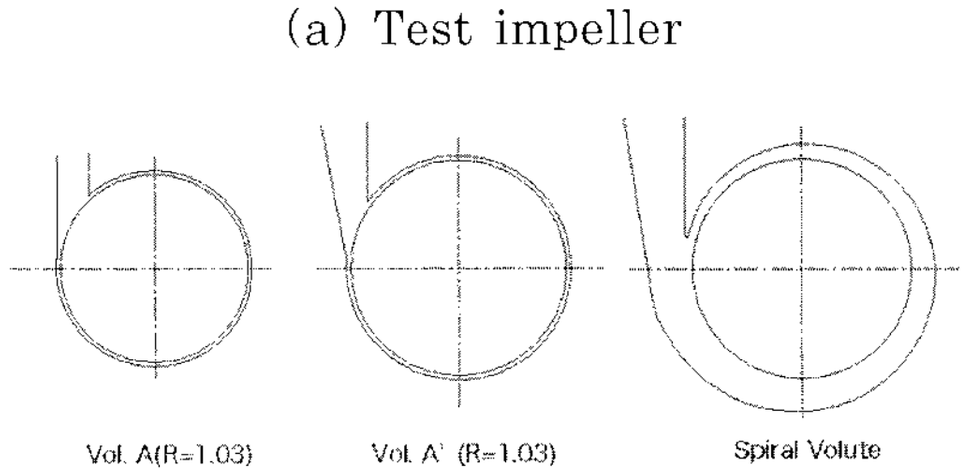

(b) casings

Fig. 2 Test impeller and casings

Fig. 3 Raw image by PIV measurement in the discharge throat region

The spiral casing has a logarithmic radius because the depth of the casing is constant. In the case of circular casing, type A has a straight channel but type A′ has an expanded diffuser channel. The radius ratio R by the outer radius r_3 of circular casings to the radius of impeller outlet r_2 has the various values that are $R=r_3/r_2$ = 1.03, 1.15, 1.3, 1.5.

The internal velocity field near the tongue area is measured by the PIV method of Choi et al.[5] A double-pulsed Nd:YAG laser sheet (20 mJ) is used as a source of illumination. The thickness of the light sheet is fixed to 0.5 mm. A CCD camera whose resolution is 1300 x 1030 pixel takes the image of the flow field from the direction perpendicular to a plane of light sheet. The intervals of the laser pulses are set to 100 μs. Particles of nylon 12 whose diameter is about 30 μm are used as tracers.

One plane in the direction perpendicular to the impeller axis are measured at middle passage width (z/b=0.5), while z is a wall-normal distance from the shroud side wall, and b is an impeller passage height (9mm).

A triggering signal is captured from the shaft of the pump, so that the PIV raw images in which the impeller blade is at the same position are collected and averaged.

Fig. 3 shows a raw image taken by present PIV system. Though there are shadows made by impeller blade and casing tongue, the discharge inlet region of the channel is taken very clearly.

2.2 Numerical methods

Unsteady numerical simulations are performed using a commercial software of ANSYS-CFX[8]. Figure 4 shows the total flow field by modeling[8] of the test pump(Fig. 4(a)) and the magnified grid view in the discharge throat(tongue) region of the test pump(Fig. 4(b)). The calculation region of the test pump consists of four parts, such as the suction pipe, discharge channel, impeller and casing, as shown in Fig. 4(a).

The total node number of the numerical grid is about 1.3×10^6 in all simulation cases. The grid parts of suction pipe and impeller are combined by the grid boundary condition of transient rotor-stator method. The same method is also used in the grid boundary between the impeller and casing.

The k-ω SST turbulent model is used. As the boundary condition in the calculation domain, average velocity is given at the inlet of the suction pipe and constant pressure is set at the outlet of the discharge pipe.

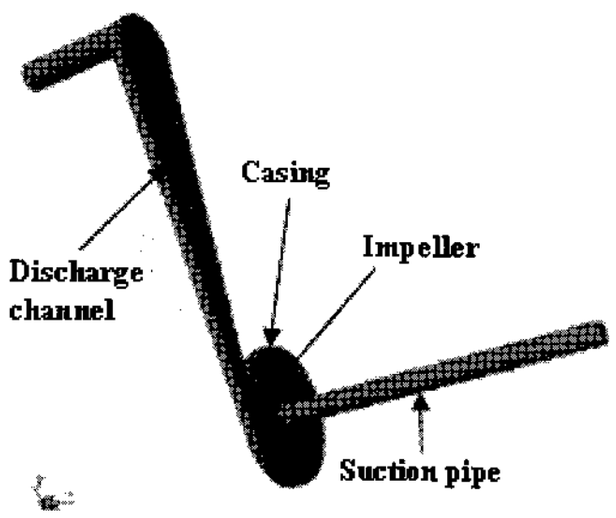

(a) Modeling of total flow field in the test pump

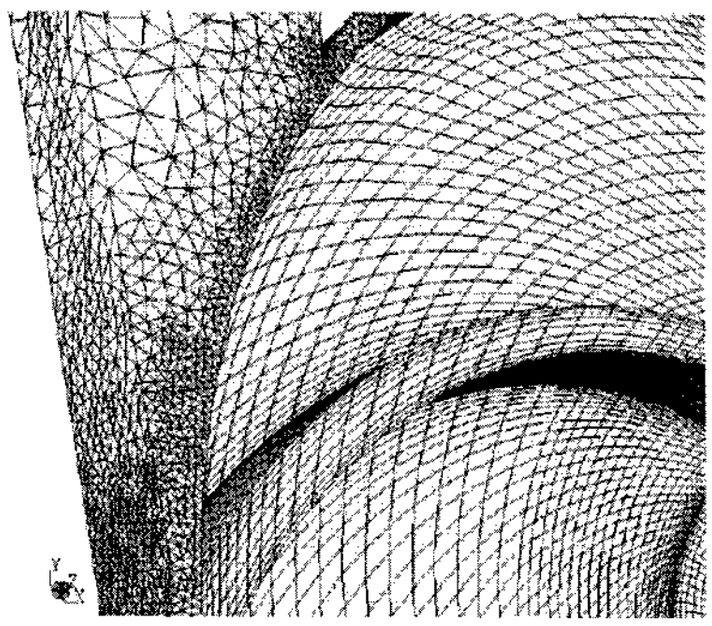

(b) Numerical grids near discharge throat

Fig. 4 Numerical grids of test pump

Fig. 5 presents the performance comparison at the best efficiency point by experiment and CFD, where the head coefficient($\psi = H/(u_2^2/2g)$) is plotted vs. the discharge coefficient($\phi = Q/A_2u_2$). where, the factors of H, u_2, g, Q and A_2 represent head, rotational speed at impeller outlet, acceleration of gravity, discharge flow rate and cross-sectional area at impeller passage outlet, respectively. The time-averaged head calculated by the CFD simulation agrees very well with the experimental result, both in the case of spiral casing and circular casing.

3. Results and discussion

3.1 Performance curves

Fig. 6 shows the performance curves with various radius of the circular casings, where the head coefficient(ψ), the power coefficient(τ), the local type number(k)[1] are plotted vs. the discharge coefficient (ϕ). The casing types A, B, C, and D have different outer radius of r_3. In the case of type A, whose radius $R=r_3/r_2=1.03$, the discharge flow rate at the best efficiency point (BEP) is $Q_{BEP} = 1.77\text{m}^3/\text{h}$, its discharge coefficient is 0.0293, the total head is $H_{BEP}=1.52\text{m}$. The local type-number(which is non-dimensional local specific speed) at the best efficiency point is $k_{BEP} = 0.275$, that is a little higher than the designed value, 0.244.

As the increase of the outer radius ratio R, the head is reduced. However, at the smallest R, type A, the highest head and best efficiency is achieved. The power coefficient τ is not changed so much by the outer radius ration. Therefore, almost the same value of the power coefficients indicates that the reason of head difference is mainly resulted from the loss in the casing.

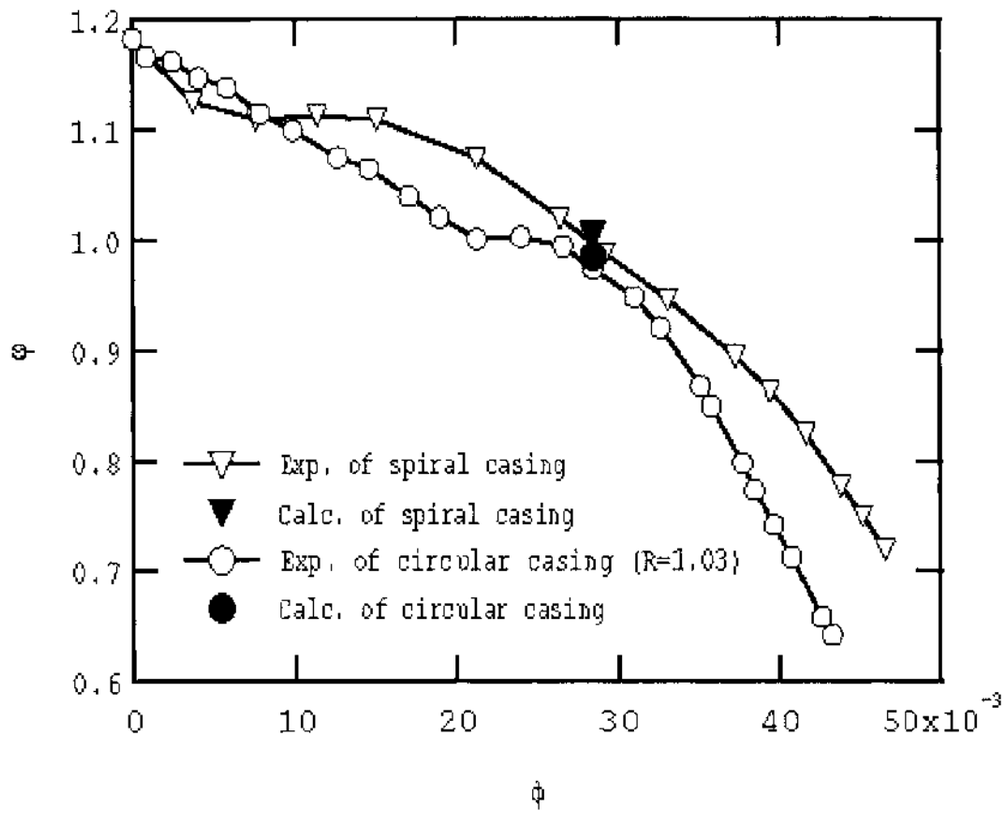

Fig. 5 Comparison of performance curves

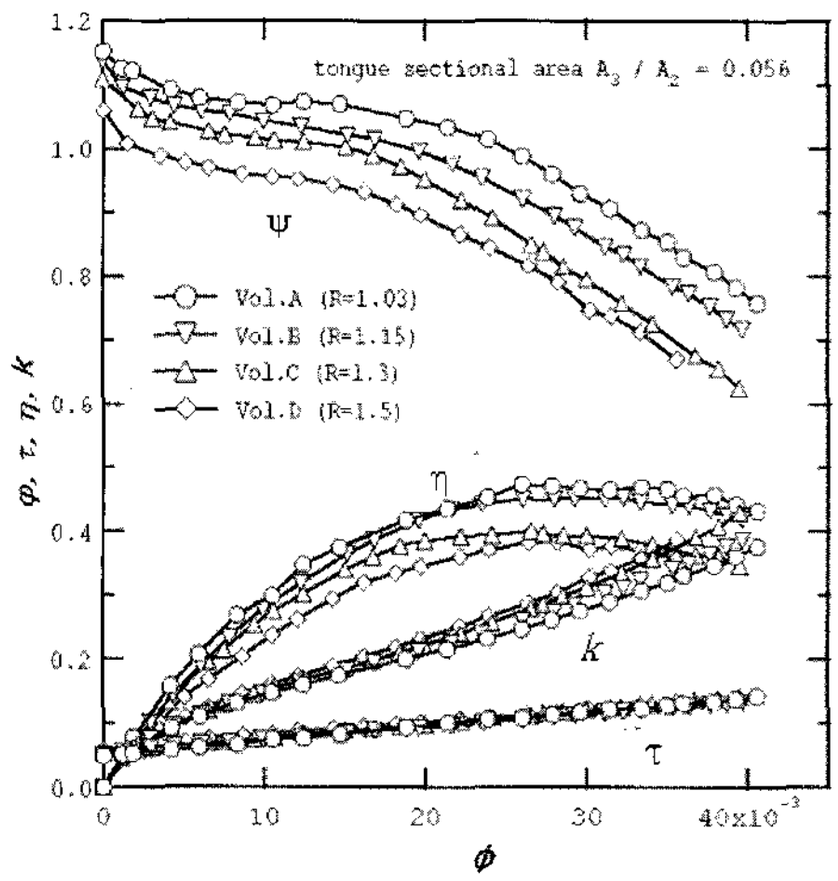

Fig. 6 Performance by outer radius ratio (experimental results)

Fig. 7 indicates the comparison of the performance curves by the casing types of spiral casing, circular casings A and A′.

The result by the spiral casing shows the higher head coefficient ψ than those of the circular casings in the almost range of the discharge coefficient ϕ. The result by the circular casing of type A′ shows the almost same head and efficiency with those of the spiral casing near the best efficiency point. However, at the excessive range of discharge coefficient, both head and efficiency are decreased. The efficiency by the casing A is a little lower than that of the type A′ in the almost whole flow rate range.

Therefore, in order to examine the reason of performance difference by the casing type in detail, flow fields of the pump both by the casing A′ and spiral casing are investigated by use of CFD analysis and PIV measurement.

3.2 Transient velocity vectors and distributions calculated by CFD

Fig. 8 shows the calculated velocity vectors in the test pump with the variation of casing type. The velocity vectors are shown on the middle cross section of z/b=0.5. The calculated discharge value is set at the best efficiency point of the experiment.

The angle ζ means the position of the impeller blade. When ζ=0 degree, the blade end tip at the impeller outlet is on the line between the center of the axis and tongue tip. As the number of the impeller blade is four, the next blade comes on that line when ζ=90 degree.

When the spiral casing is installed in the pump as shown in Fig. 8(a), there are separated vortices at the inlet of the impeller, and very strong through flow goes downstream along to the both suction and pressure sides of the blade. In the center region of the blade passage, strong secondary flow occurs to the pressure side of the blade. This is a typical flow pattern in the low type number impeller.[5]

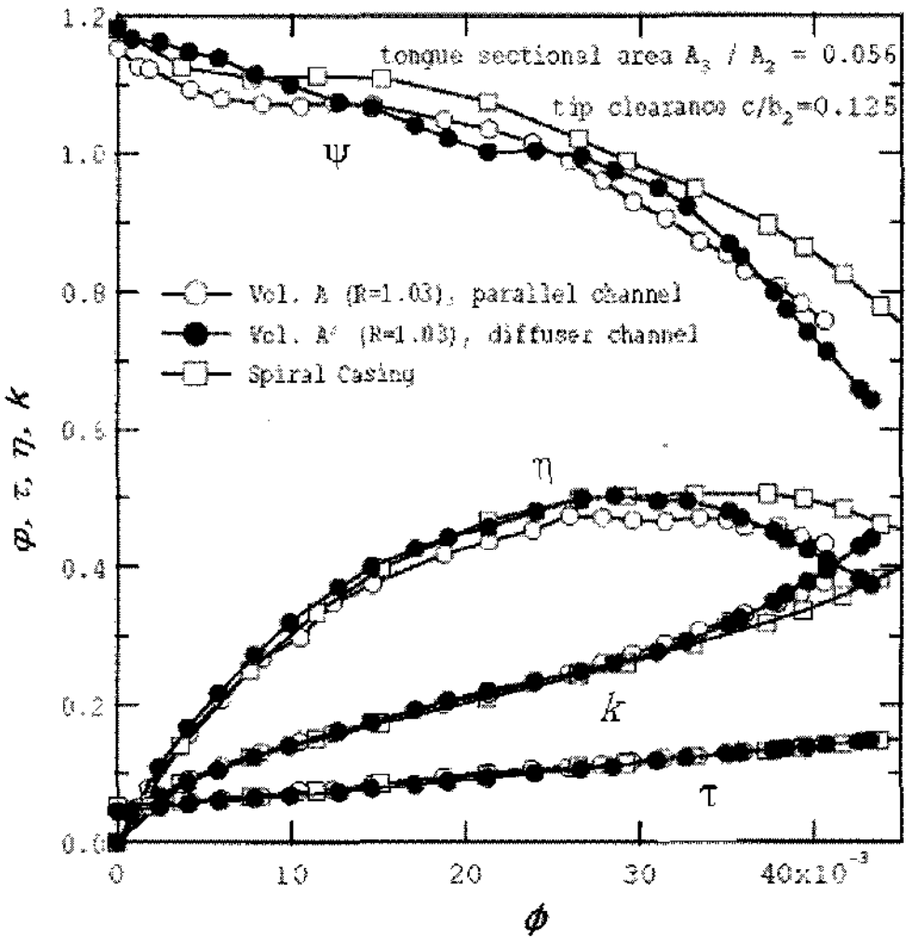

Fig. 7 Performance change by casing types(experimental results)

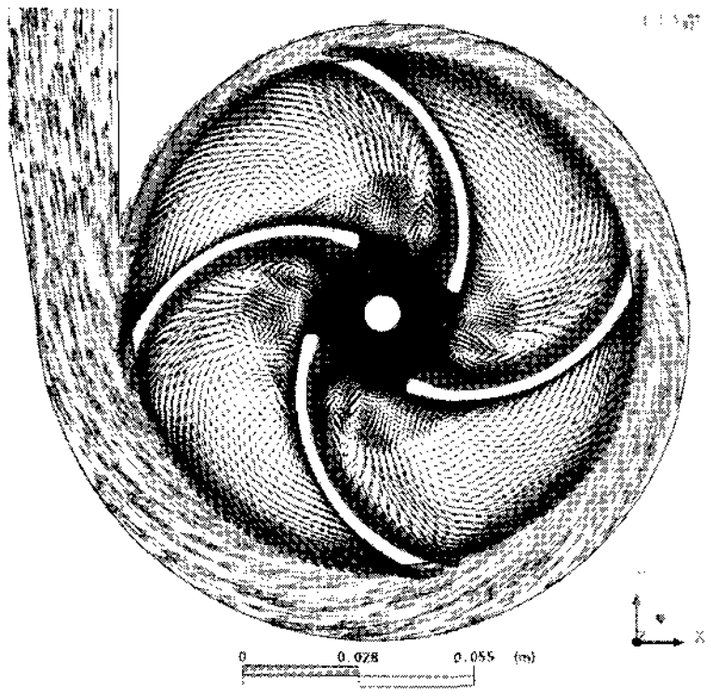

(a) Spiral casing (ζ=67 deg.)

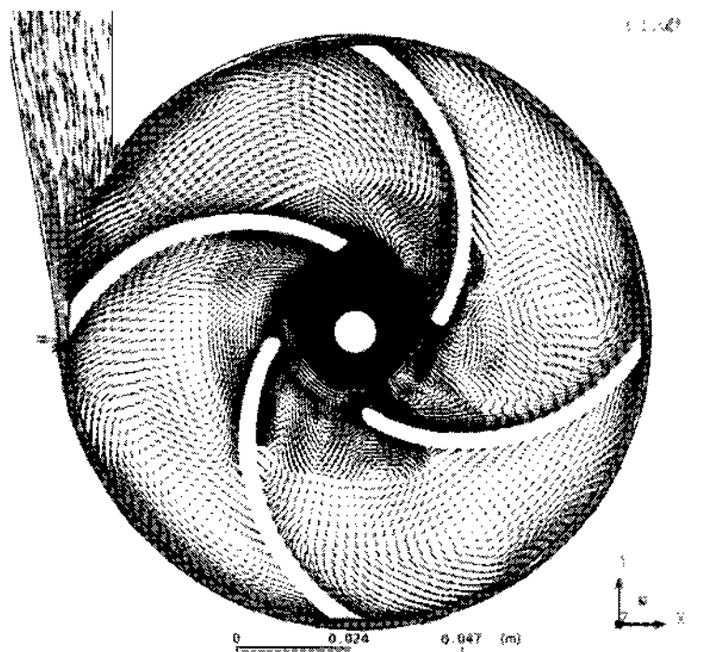

(b) Circular casing A′ (ζ=48 deg.)

Fig. 8 Transient velocity vectors by CFD.

The flow in the pump by circular casing A′ shows more complicated flow pattern (Fig. 8(b)) than that by spiral casing(Fig. 8(a)). There are large vortexes in the center of each impeller channels except for the channel near the discharge throat region, as well as strong secondary flow in all blade passages. The flow at the outlet of the impeller goes out only at the throat region and the flow does not go out from the impeller outlet in the other region. Even at the best efficiency point, the flow in the pump by circular casing is asymmetric. Also the unsteadiness is much larger than that by spiral casing.

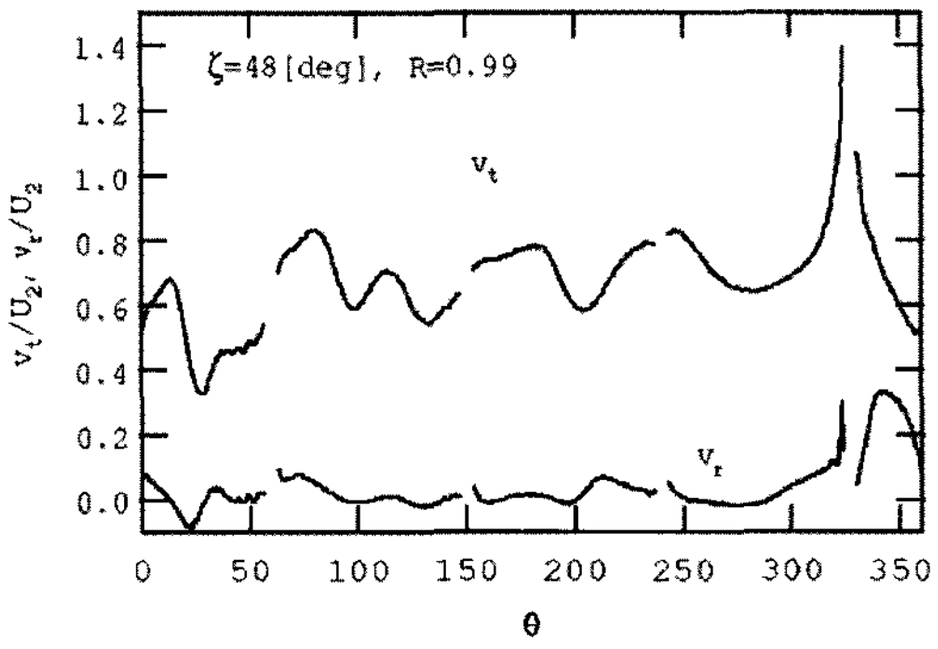

(a) ζ=48 deg.

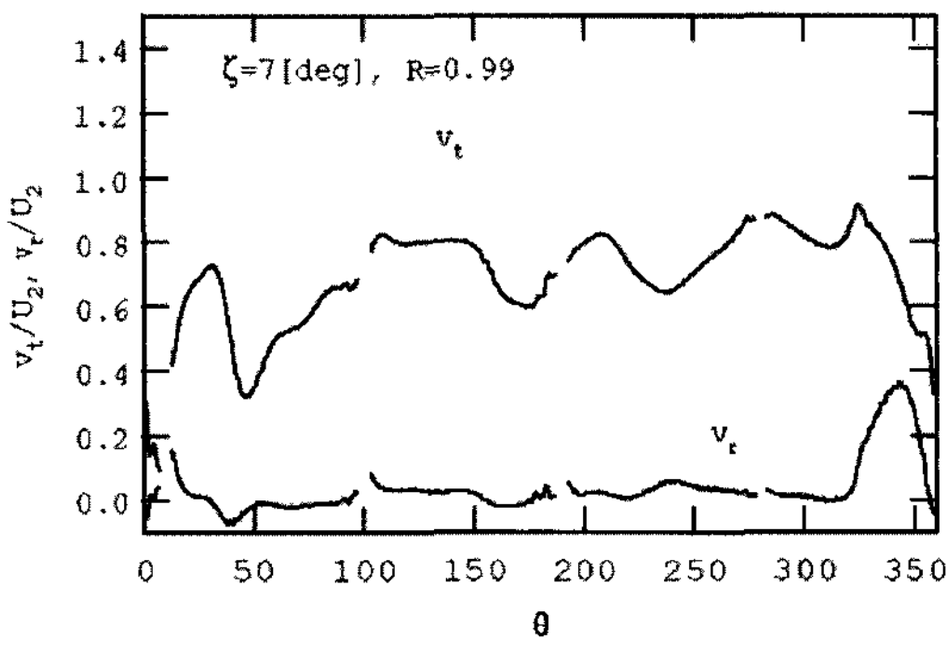

(b) ζ=7 deg.

Fig. 9 Transient velocity distribution in the circular casing A' (CFD)

Fig. 9 shows the calculated velocity distribution at the impeller outlet of $R=r/r_2=0.99$ with the change of blade location ζ of the test impeller when circular casing A′ is adopted. Discontinuity region in the velocity distribution means the location of impeller blade.

In the Fig. 9(a), when the blade is approaching to the discharge throat region of the casing, the tangential velocity v_t becomes so large that it is more than the rotational speed of impeller U_2. However, this high tangential velocity disappears after the blade passed the volute tongue region.

Moreover, the radial velocity v_r becomes

remarkable only near the region of the discharge throat from θ=320 to 360 degree, while volute angle θ is the angle from the volute tongue to a position in the clockwise direction along the outlet of the impeller. However, in the almost regions of impeller outlet except for the discharge throat region, radial velocity is constant regardless of the blade position.

Therefore, It is clear that the flow in the impeller outlet is strongly controlled by the circular casing because the velocity distribution almost does not affected by the position of the impeller blades.

3.3 Transient velocity distribution in the casing measured by PIV

Fig. 10 shows the measured transient velocity distribution at the discharge throat of the circular casing by PIV. The velocity measurement is conducted on the plane of z/b=0.5 in the range of the best efficiency point. The data are collected at the radius ratio of $R=r/r_2$=1.01.

Fig. 10(a) shows the radial velocity distribution divided by the rotational speed of impeller outlet U_2. Radial velocity distribution at the pressure and suction sides of the blade is relatively very high as the blade is moving from ζ =60, 75 and 0 degree. From the angle θ =-40 to 0 degree, where is the throat region of the casing, there exits almost outward flow, which agrees with the CFD results as shown in Fig. 9.

The tangential velocity distribution indicates that there always exists relatively high tangential velocity about $v_t = 0.9U_2$ around the position of θ=-35 degree as shown in Fig. 10(b). However, the measured tangential velocity is not so large as that in the CFD result at the radius ratio of $R=r/r_2$=0.99 as shown in Fig. 9(a).

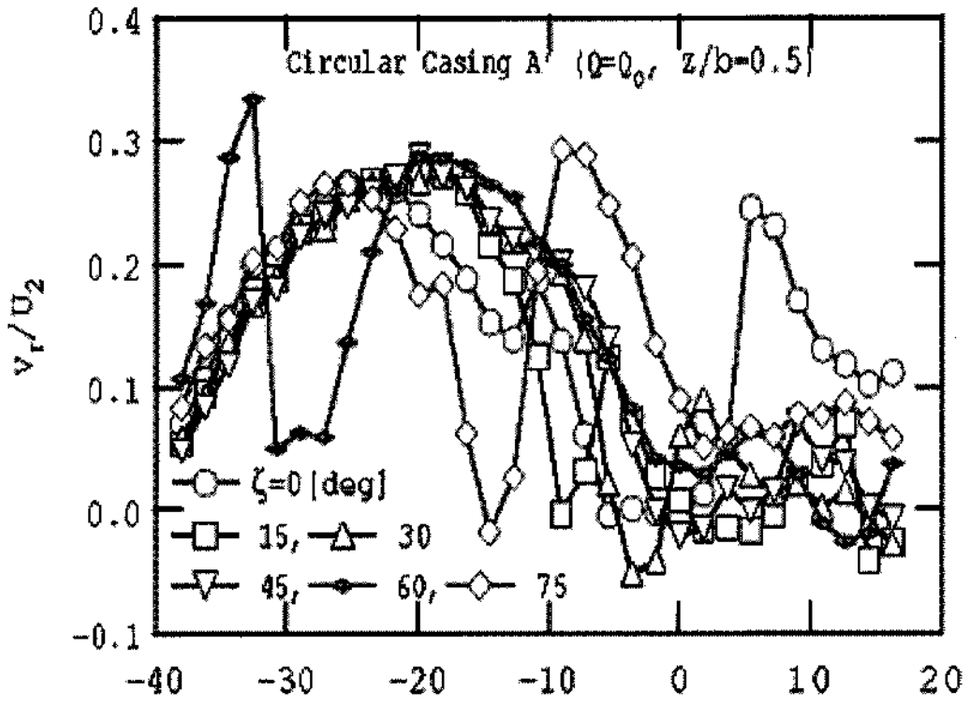

(a) Radial velocity distribution

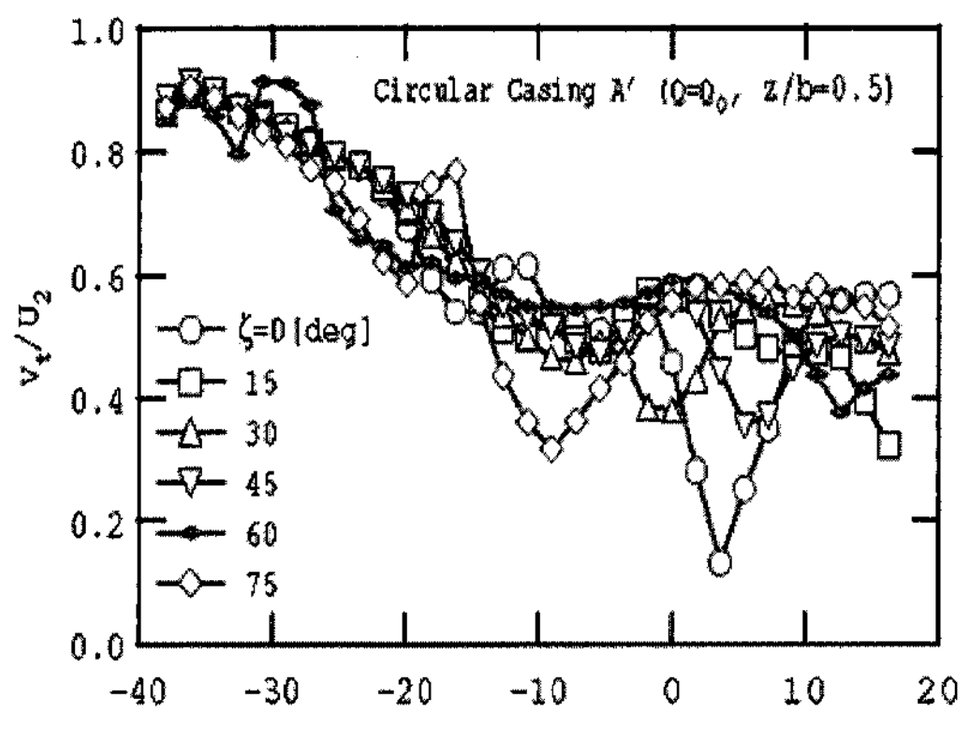

(b) Tangential velocity distribution

Fig. 10 Transient velocity distribution by PIV measurement

The reason of relatively low tangential velocity from PIV measurement is conjectured that as the PIV data are measured at the casing passage(R=1.01), the flow make mixture during the flow goes into the casing from impeller outlet, and then the flow mixture may make the distribution smoother in case of experiment.

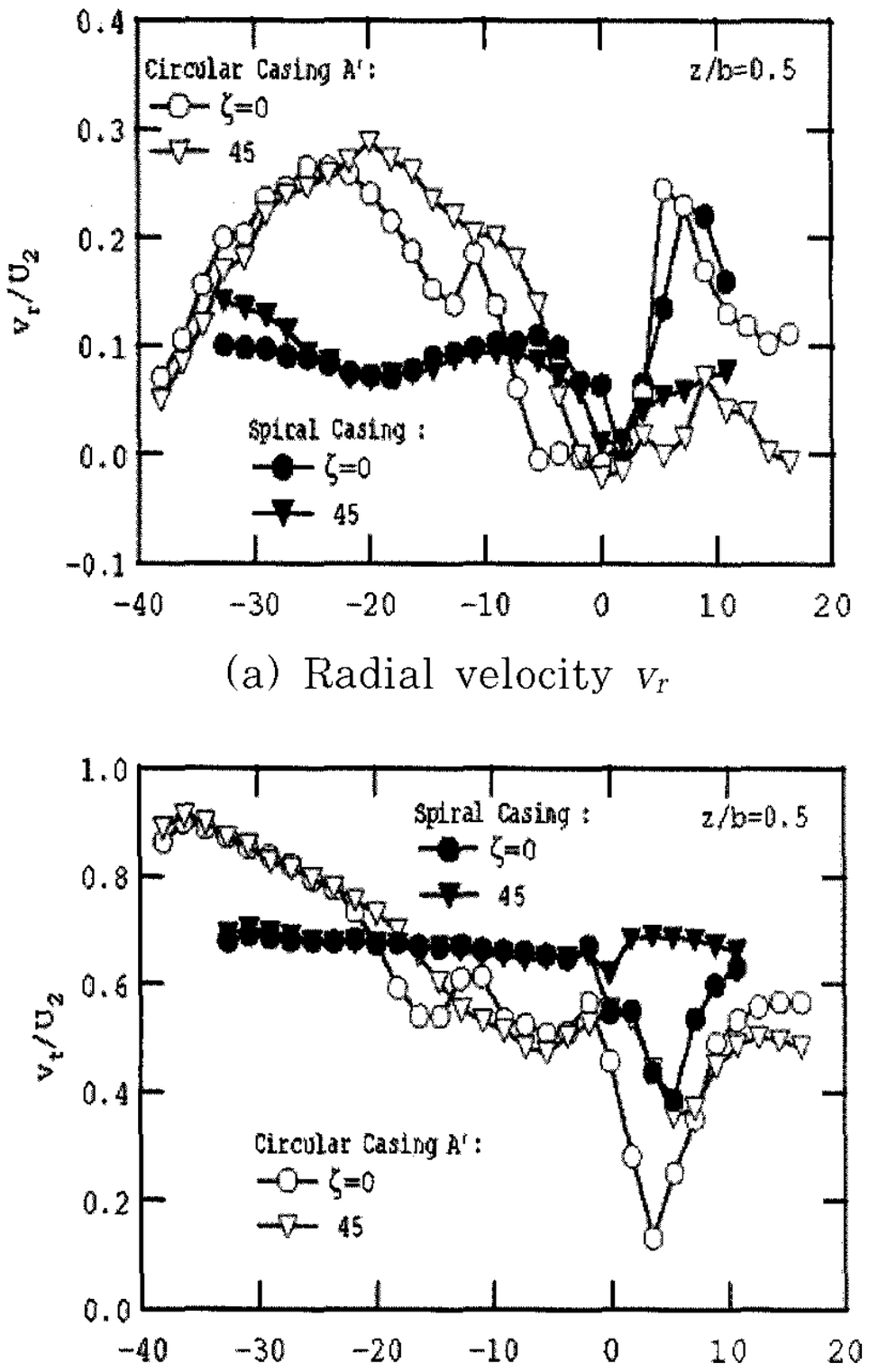

(a) Radial velocity v_r

(b) Tangential velocity v_t

Fig. 11 Comparison of velocity distribution by the casing type (PIV)

Fig. 11 presents the comparison of measured velocity distributions near the discharge throat region in the pump according to the spiral and circular casing types. In the spiral casing, the radial and tangential velocity distributions becomes flat except for just near the tongue region. However, considerable velocity changes with the variation of volute location of θ can be checked in the case of installing circular casing A′ as shown in Fig. 11.

Therefore, this result reveals that velocity by circular casing in the region of discharge throat near volute tongue has higher values of radial velocity v_r, as well as the unsteadiness than those by spiral casing.

3.4 Time averaged velocity distribution

Fig. 12 shows the time-averaged velocity distribution calculated by CFD. In the case of spiral casing, the radial and tangential velocity distributions are almost constant with the variation of the volute angle θ. On the other hand, in the case of circular casing, the radial and tangential velocities increase only at the region of discharge throat but almost flat velocity distribution exists at the other region. The high velocity near the discharge throat should be suppressed to keep the stable operation of the pump without radial thrust.

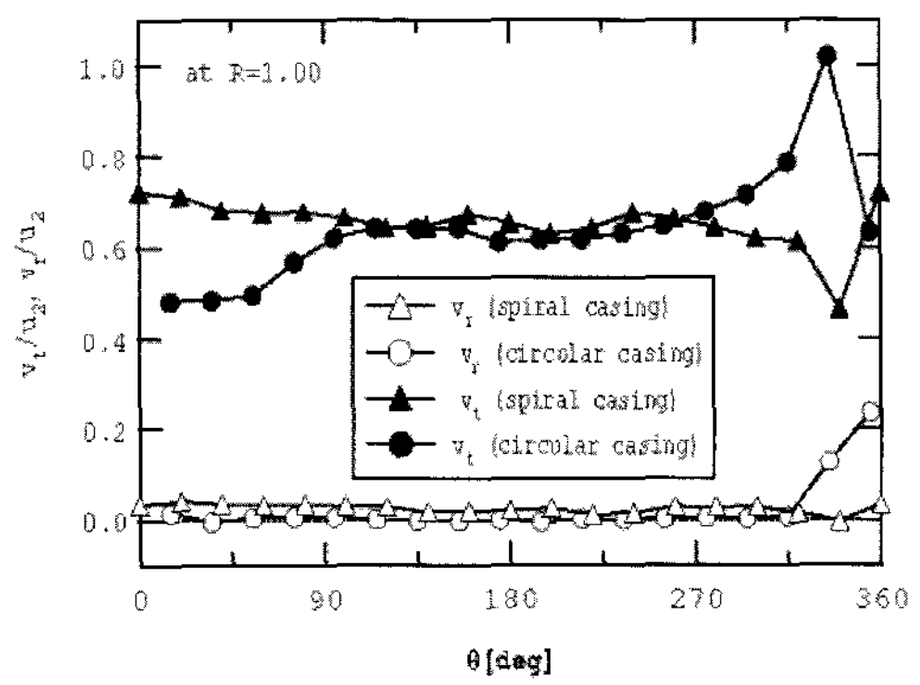

Fig. 12 Time averaged velocity distribution by CFD

4. Conclusions

The internal flows of a low specific speed centrifugal pump with circular and spiral casings are analyzed by PIV measurement and CFD calculation. From the results of the present study, the following conclusions have been obtained.

1. Time-averaged radial and tangential velocity distributions in the spiral casing

are almost constant with the change of the volute position. However, in the circular casing, the radial and tangential velocities increase only at the region of discharge throat but almost flat velocity distributions exist at the other region.

2. The flow in the impeller outlet is strongly controlled by the circular casing because the velocity distribution at the impeller outlet almost does not affected by the position of the impeller blades.

3. The flow in the pump by circular casing shows very complicated flow pattern than that by spiral casing. There are large vortexes and strong secondary flow in the blade passages. Even at the best efficiency point, the flow in the impeller with circular casing is asymmetric.

4. Circular casing has high applicability in the range of low specific speed because of its simple configuration and almost constant velocity distributions in the casing passage. However, strong velocity unsteadiness in the region of discharge throat near volute tongue should be suppressed to keep the stable operation of the pump without radial thrust.

Reference

[1] Stepanoff, A. J., "Centrifugal and Axial Flow Pumps," 2nd ed., pp. 69-89, John Wiley and Sons, 1957.

[2] Kurokawa, J., Matsui, J., Kitahora, T., Saha, S. L., Matsumoto, K. and Tsutsui, A., "Performance of Very Low Specific Speed Impeller," Turbomachinery (in Japanese), Vol. 25, No.7, pp. 337-345, 1997.

[3] Kurokawa, J., Matsumoto, K., Yao, W., Matsui, J. and Hiroshi, I., "Study on Optimum Configuration of a Volute Pump of Very Low Specific Speed," Trans. JSME, Series B (in Japanese), Vol. 66, No. 644, pp.1132-1139, 2000.

[4] Matsumoto, K., Kurokawa, J., Matsui, J. and Hiroshi, I., "Performance Improvement and Peculiar Behavior of Disk Friction and Leakage in Very Low Specific Speed Pumps," Trans. JSME, Series B (in Japanese), Vol. 65, No. 640, pp.4027-4032, 1999.

[5] Choi, Y-D., Nishino, K, Kurokawa, J. and Matsui, J., "PIV Measurement of Internal Flow Characteristics of Very Low Specific Speed Semi-open Impeller," Experiments in Fluids, Vol. 37, pp. 617-630, 2004.

[6] Choi, Y-D., Kurokawa,J., Matsui,J., "Performance and Internal Flow Characteristics of a Very Low Specific Speed Centrifugal Pump," J. Fluids Eng.,Vol. 128, pp. 341-348 , 2006.

[7] Choi,Y-D., Kagawa, S. and Kurokawa J., "Influence of Circular Casing on the Performance of Very Low Specific Speed Centrifugal Pump," Journal of Fluid Machinery, Vol. 9, No. 1, pp. 32-39, 2006.

[8] ANSYS Inc.,"ANSYS-CFX Documentation," Ver. 11, http://www. ansys.com, 2007.

Author Profile

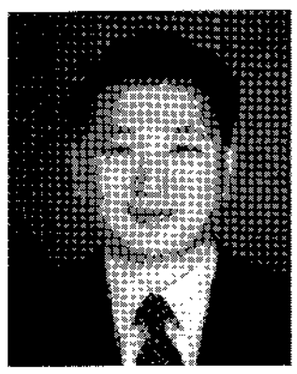

Young-Do Choi

He received his B.E. and M.Eng. degrees from Korea Maritime University, and his Dr.Eng. from Yokohama National University, Japan. He is currently a researcher in the Industry- Academic Cooperation Foundation at Korea Maritime University in Busan, Korea. His research interests include new & renewable energy, fluid machinery, PIV, CFD and flow visualization.